Polymer Chemistry

ROYAL SOCIETY OF CHEMISTRY

PAPER

View Article Online
View Journal | View Issue

Cite this: *Polym. Chem.*, 2020, **11**, 5181

Single-chain crosslinked polymers *via* the transesterification of folded polymers: from efficient synthesis to crystallinity control†

Daiki Ito,[a] Yoshihiko Kimura,[a] Mikihito Takenaka,[b,c] Makoto Ouchi[a] and Takaya Terashima*[a]

Received 25th May 2020,
Accepted 7th July 2020

DOI: 10.1039/d0py00758g

rsc.li/polymers

Herein we report efficient synthetic systems of single-chain crosslinked polymers *via* the intramolecular transesterification of folded random copolymers in organic media and the unique crystallization behavior of their crosslinked polymers. For this purpose, we designed random terpolymers comprising octadecyl methacrylate (ODMA), 2-hydroxyethyl methacrylate, and methyl acrylate (MA). The copolymers self-folded in octane *via* the association of the hydroxyl groups to form reverse micelles; the micelles were intramolecularly crosslinked by scandium-mediated transesterification of the MA units with the hydroxyl groups to give polymer nanoparticles bearing multiple octadecyl groups. This system affords efficient synthesis of various single-chain crosslinked polymers with controlled molecular weight at a relatively high concentration of up to 50 mg mL^{-1}. Additionally, the crystallinity of these ODMA-based copolymers can be controlled by the crosslinking degree; the crystallinity and melting temperatures of the octadecyl groups gradually decreased as the intramolecular crosslinking of the copolymers proceeded. Thus, controlling the intramolecular crosslinking of polymers is one possibility to tune the crystallinity of polymer materials.

Introduction

Crosslinked globular polymers serve as interesting functional nanomaterials with unique physical properties and compartments and are thus utilized for various applications as nanocapsules, delivery vessels, dispersants, and coatings, among many others. Several types of crosslinked polymers have been developed by using controlled polymerization and crosslinking techniques as follows: microgel star polymers,[1–8] core or shell-crosslinked block copolymer micelles,[9–13] and single-chain crosslinked polymers and single-chain polymer nanoparticles (SCPNs).[14–33] Microgel star polymers and crosslinked block copolymer micelles are obtained from the intermolecular crosslinking of polymers. In contrast, single-chain crosslinked polymers are prepared by the intramolecular crosslinking of polymer chains *via* physical self-assembly (*e.g.*, by hydrogen-bonding,[19,20] metal coordination,[21,22] and molecular recognition[23]) or covalent bond formation (*e.g.*, by thiol–ene and thiol–yne,[24] Diels–Alder,[25] photodimerization,[26] olefin metathesis,[27] radical addition,[28,29] imine,[30,31] disulfide,[32] and polymerization[33]). In principle, crosslinking of single polymer chains is efficient at controlling the molecular weight of crosslinked polymers as desired because well-defined precursors prepared by controlled polymerization can be unimolecularly transformed into products. However, selective crosslinking of single polymer chains often requires dilute conditions ($\lesssim$0.1 mg mL^{-1}) to suppress intermolecular crosslinking into multichain aggregates and network polymers. To overcome this issue, covalent crosslinking of autonomously folded polymers and unimer micelles has been investigated as a high-throughput approach to single-chain crosslinked polymers and related polymers in solutions.[28,29,31]

We have recently developed self-assembly systems of amphiphilic random copolymers bearing hydrophilic poly(ethylene glycol) (PEG) and hydrophobic alkyl groups as side chains in water, organic media, and the solid state.[34–38] Typically, random copolymers carrying PEG and dodecyl groups induce chain folding in water *via* the association of the hydrophobic pendants to form unimer or multichain micelles with globular and compact structures. Their micelles are selectively obtained even at a relatively high concentration (~60 mg mL^{-1}) by controlling the degree of polymerization (DP) and composition

[a]*Department of Polymer Chemistry, Graduate School of Engineering, Kyoto University, Katsura, Nishikyo-ku, Kyoto 615-8510, Japan. E-mail: terashima.takaya.2e@kyoto-u.ac.jp*
[b]*Institute for Chemical Research, Kyoto University, Gokasho, Uji, Kyoto 611-0011, Japan*
[c]*RIKEN Spring-8 Center, Sayo-cho, Sayo-gun, Hyogo 679-5148, Japan*

†Electronic supplementary information (ESI) available: Experimental details, and characterization by SEC, NMR, SANS, and DSC. See DOI: 10.1039/d0py00758g

(hydrophilic/hydrophobic balance) of the copolymers.[34–36] This is because the hydrophobic pendants are accumulated inside and isolated by the hydrophilic shell of multiple PEG chains. As a result, unimer micelles of random copolymers bearing hydrophilic PEG and hydrophobic olefin or amino groups can be intramolecularly crosslinked by a radical reaction or imine bond formation in water to produce single-chain crosslinked polymers without forming large aggregates (Scheme 1b).[28,29,31] Additionally, amphiphilic random copolymers are capable of reversible folding in aqueous and organic media by designing side chains.[37,38] Typically, random copolymers bearing PEG and octadecyl groups not only folded into micelles with hydrophobic cores in water but also formed reverse micelles with hydrophilic PEG cores in hexane.[38] This result motivated us to use reverse micellization for the efficient synthesis of single-chain crosslinked polymers that are totally hydrophobic and dissolved only in organic solutions; crosslinking of folded amphiphilic polymers has usually been investigated in aqueous media for water-soluble polymer nanoparticles.

Given these backgrounds, we herein developed synthetic systems of single-chain crosslinked polymers *via* the intramolecular crosslinking of random copolymer reverse micelles in organic media (Scheme 1a). To achieve both reverse micellization of random copolymers and intramolecular crosslinking of their micelles, we focused on acrylate-selective transesterification of methacrylate/acrylate random copolymers[39] as a crosslinking method. For this, random copolymers comprising hydrophobic octadecyl methacrylate (ODMA) or related methacrylates, hydrophilic 2-hydroxyethyl methacrylate (HEMA), and methyl acrylate (MA) units were designed.

Transesterification is effective for the site-selective and pinpoint functionalization of well-controlled poly(meth)acrylates because of the unique reactivity and selectivity of the pendant ester groups.[39–43] If methacrylate (RMA)/methyl acrylate (MA) random copolymers are transesterified with metal catalysts (*e.g.*, Ti(O*i*-Pr)$_4$) and alcohols (R^1OH), the MA units are preferentially transformed into the corresponding alkyl acrylate (R^1A) units to give RMA/R^1A random copolymers.[39] This is because the main chain carbons adjacent to the MA units have no α-methyl groups, and the MA carbonyl groups are less sterically hindered than the other methacrylate counterparts. Therefore, ODMA/HEMA/MA random copolymers satisfy the following requisites: (1) the copolymers self-fold into reverse micelles in hexane, in which the hydroxyl groups are accumulated inside and the multiple octadecyl groups stabilize the folded structures. (2) The MA units are intramolecularly and selectively transesterified with the HEMA hydroxyl groups to induce covalent crosslinking of the reverse micelles into single-chain crosslinked polymers.

As expected, the reverse micellization afforded unimolecular crosslinking even at a relatively high concentration (~50 mg mL^{-1}). The efficient intramolecular crosslinking of the copolymers was confirmed by size-exclusion chromatography coupled with multiangle laser light scattering (SEC-MALLS). The molecular weight of the crosslinked polymers was directly controlled by the random copolymer precursors that are prepared by living radical polymerization. This system is further applicable to the synthesis of various crosslinked polymers comprising dodecyl methacrylate (DMA), methyl methacrylate (MMA), and related monomers. Additionally, single-chain crosslinked ODMA copolymers showed unique crystallinity of the octadecyl pendants in the solid state. The crystallinity gradually decreased as the intramolecular crosslinking of the copolymers proceeded, meaning that the pendant crystallinity

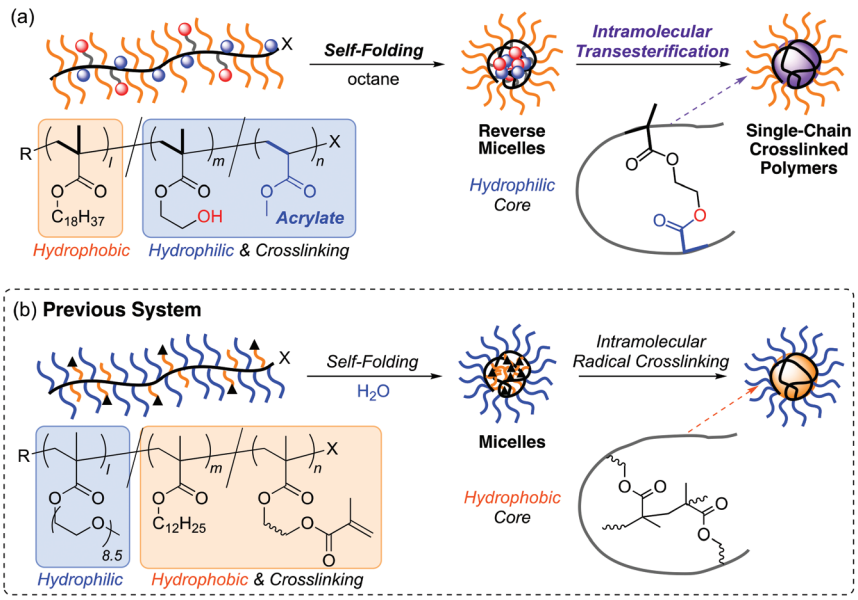

Scheme 1 Single-chain crosslinked polymers (a) *via* the intramolecular transesterification of reverse-folded micelles in organic media or (b) *via* the radical crosslinking of folded micelles in water.

is controllable by the crosslinking degree. Thus, intramolecular transesterification of these common methacrylate/acrylate random copolymers provided efficient synthetic methodologies for various hydrophobic polymer nanoparticles and crystallization control techniques for polymer materials.

Results and discussion

Polymer design and synthesis

We designed various methacrylate/acrylate random copolymers bearing hydroxyl pendants (**P1–P11**, Scheme 2) as precursors for single-chain crosslinked polymers. Random copolymers bearing octadecyl and hydroxyl pendants and methyl acrylate units (**P1–P5**) were prepared by ruthenium-catalyzed living radical copolymerization of ODMA, HEMA, and MA. The polymer design involves (1) reverse micellization in organic media, (2) crosslinking by acrylate-selective transesterification, and (3) the production of crystalline polymer materials. The degree of polymerization (DP) and the content of the crosslinking units (HEMA and MA) were varied (Table 1). **P1–P4** had different DP (67–280) with an almost constant content of the linking units ($m + n$ = ~40 mol%), while **P5** had a high content of the linking units ($m + n$ = 67 mol%) with 135 DP: ODMA/HEMA/MA = 160/55/65 (**P1**), 140/40/55(**P2**), 95/27/35 (**P3**), 40/15/12 (**P4**), and 45/65/25 (**P5**).

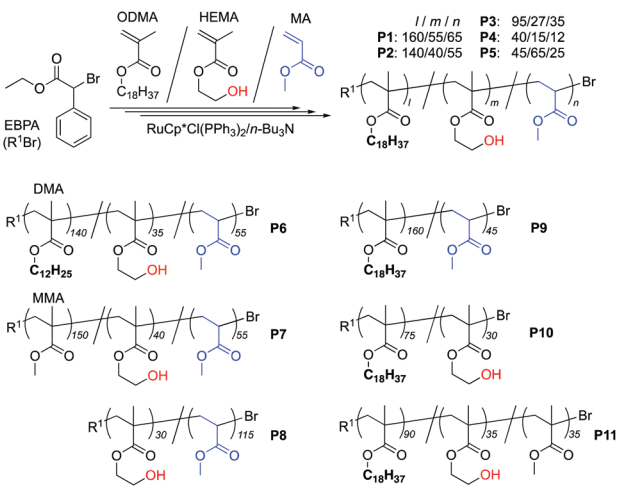

Scheme 2 Design and synthesis of hydroxyl-functionalized methacrylate/methyl acrylate random copolymers and related copolymers (**P1–P11**) as precursors for single-chain crosslinked polymers.

For **P1–P5**, ODMA, HEMA, and MA were copolymerized with a ruthenium catalyst [RuCp*Cl(PPh_3)$_2$/n-Bu_3N][39] and a bromide initiator (ethyl α-bromophenylacetate: EBPA) in toluene/1,4-dioxane (1/1, v/v) at 80 °C. In all the cases, the three monomers were simultaneously consumed to produce well-controlled ODMA/HEMA/MA copolymers with a narrow molecular weight distribution [**P1–P5**, M_w/M_n < 1.2 was determined by size exclusion chromatography (SEC) in THF with PMMA standard calibration, Table 1]. The content of the three monomer units in the copolymer (F_{cum}) was almost constant along the polymer chain (Fig. S1†), calculated from the monomer conversion. This importantly means that these copolymers consist of a random monomer sequence along the polymer chain without any biased sequence distribution like gradient copolymers.[43] The products (**P1–P5**) were purified by preparative SEC or precipitation into methanol to remove catalyst residues and unreacted monomers. The DP, composition, and number-average molecular weight of **P1–P5** were determined by ^{1}H NMR. To evaluate the crosslinking behavior of the products by transesterification, the absolute weight-average molecular weight of the copolymers was also determined by SEC-MALLS in THF.

In addition to octadecyl-bearing copolymers, random copolymers comprising dodecyl methacrylate (DMA) or methyl methacrylate (MMA) (**P6**, **P7**) were synthesized (Scheme 2, Table 1). DP (230, 245) and the HEMA/MA content (~40 mol%) were set to be almost the same values as those of **P2**. An acrylate-based precursor (**P8**) was prepared with HEMA and MA. Three control samples were also prepared: an ODMA/MA copolymer (**P9**) without HEMA units, an ODMA/HEMA copolymer (**P10**) without MA units, and an ODMA/HEMA/MMA copolymer (**P11**) containing MMA instead of MA (Table S1†).

Table 1 Synthesis and characterization of RMA/HEMA/MA random copolymers[a]

Polymer	RMA	Time (h)	Conv.[b] (%)	DP[c]	$l/m/n_{obsd}$ [c] (RMA/HEMA/MA)	m/n (linking) (mol%)	M_n [d] (SEC)	M_w/M_n [d] (SEC)	M_n [c] (NMR)	M_w [e] (MALLS)
P1	ODMA	24	71/83/44	280	160/55/65	20/23	64 200	1.14	67 200	76 800
P2	ODMA	66	64/80/52	235	140/40/55	17/23	53 300	1.18	57 600	67 700
P3	ODMA	24	74/87/49	157	95/27/35	17/22	40 300	1.12	38 900	44 900
P4	ODMA	72	37/53/31	67	40/15/12	22/18	16 800	1.14	16 800	18 000
P5	ODMA	48	35/58/26	135	45/65/25	48/19	28 600	1.14	26 100	29 400
P6	DMA	60	64/77/38	230	140/35/55	15/24	43 600	1.16	45 200	51 000
P7	MMA	48	74/83/47	245	150/40/55	16/23	28 800	1.19	25 200	31 400
P8	—	48	—/78/40	145	—/30/115	21/79	17 000	1.11	14 000	15 000

[a] Conditions: $[RMA]_0/[HEMA]_0/[MA]_0/[EBPA]_0/[RuCp^*Cl(PPh_3)_2]_0/[n\text{-}Bu_3N]_0$ = 1600/440/1160/8/0.8/8 (**P1**), 1500/400/1100/10/1/10 (**P2**), 1600/440/1160/16/1.6/16 (**P3**), 1125/300/825/15/1.5/15 (**P4**), 1280/1120/1200/12/1.2/12 (**P5**), 1500/375/1125/10/1/10 (**P6**), 3200/800/2000/20/2/20 (**P7**), and 0/750/6750/25/2.5/25 (**P8**) mM in toluene/1,4-dioxane (1/1, v/v) at 80 °C. [b] Conversion (RMA/HEMA/MA) determined by ^{1}H NMR with tetralin as an internal standard. [c] DP of RMA (l), HEMA (m), MA (n) and M_n of the copolymers determined by ^{1}H NMR. [d] Determined by SEC in THF with PMMA standard calibration. [e] Absolute weight-average molecular weight determined by SEC-MALLS in THF.

Reverse micellization

Generally, intramolecular crosslinking of polymers is conducted under dilute conditions (<0.1 wt%) to prevent intermolecular crosslinking of multiple polymer chains.[15–18] However, hydroxyl- and octadecyl-bearing random copolymers are expected to form reverse unimer micelles *via* the association of the hydroxyl groups in organic media. Reverse micellization would efficiently afford the intramolecular crosslinking *via* transesterification at a relatively high concentration (>1 wt%). Thus, the structure of an octadecyl-bearing **P2** in octane was examined by dynamic light scattering (DLS) and small angle X-ray scattering (SAXS). Octane was selected owing to its high boiling temperature that allows transesterification at high temperature. **P2** was homogeneously dissolved in octane to have unimodal DLS size distribution with a small hydrodynamic radius (R_h = 5.4 nm, Fig. 1a). Analyzed by SAXS, **P2** had a spherical and compact structure in octane different from that in THF (Fig. 1b). In the double logarithm SAXS profiles, the scattering intensity around the q range of 1–4 nm^{-1} in octane decreased with the slope of about −4. Determined by the Guinier plots (Fig. S2†), the radius of gyration of **P2** in octane (R_g = 3.4 nm) was smaller than that in THF (R_g = 5.2 nm). These results indicate that **P2** forms micelles in octane.

Single-chain crosslinked polymers *via* intramolecular transesterification

Various metal alkoxides and Lewis acid catalysts were examined for the transesterification of a hydroxyl- and dodecyl-bearing **P6** in octane. The efficiency of intramolecular transesterification was evaluated by the consumption of the MA units and the SEC peak shift of the products to a low molecular weight. Here, six kinds of catalysts employed for transesterification, direct esterification, and related reactions were investigated: $Ti(Oi\text{-}Pr)_4$, $FeCl_3$, $Sc(OTf)_3$, $Y(OTf)_3$, $Hf(OTf)_4$, and $La(OTf)_3$.[43–47]

P6 (M_n = 43 600, M_w/M_n = 1.16) was treated with these six catalysts in octane at 120 °C for 48 h ([catalyst] = 1.0 mM, [**P6**] = 10 mg mL^{-1}); the products were analyzed by ^1H NMR and SEC (Fig. 2 and S5†). In all the cases, the MA units of **P6** were consumed *via* transesterification with the hydroxyl groups, while the efficiency of the intramolecular crosslinking depended on the catalyst species. $Sc(OTf)_3$ and $Hf(OTf)_4$ catalyzed intramolecular transesterification more efficiently than the others to achieve 40% conversion of the MA units (Table 2). The SEC curves of the products clearly shifted to a low molecular weight, keeping narrow molecular weight distribution (Fig. 2c and e). The absolute weight-average molecular weight (M_w) of the product crosslinked using $Sc(OTf)_3$ was relatively close to that of **P6** (Tables 1 and 2). This indicates that intramolecular crosslinking of **P6** mainly proceeds with this catalytic system in octane. In contrast, $Ti(Oi\text{-}Pr)_4$, $FeCl_3$, $Y(OTf)_3$, and $La(OTf)_3$ induced just 10% conversion of the MA units. These products showed a small SEC peak shift to low molecular weight and/or large molecular weight parts derived from the intermolecular crosslinking of polymers. This is probably because of the low activity for transesterification, low solu-

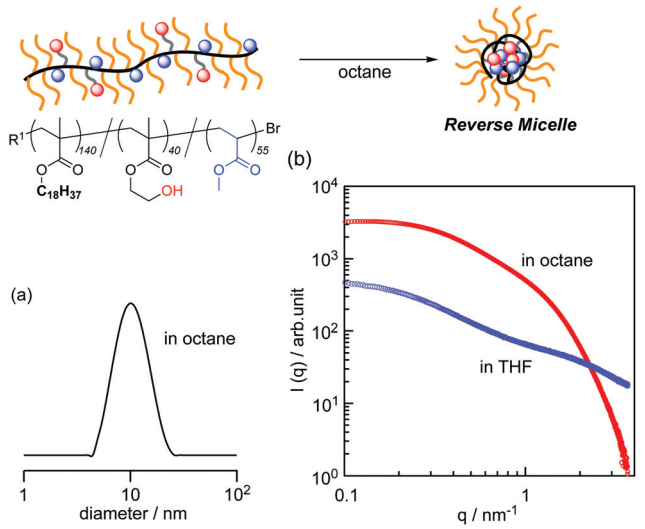

Fig. 1 (a) DLS intensity size distribution of **P2** in octane at 25 °C and (b) SAXS profiles of **P2** in octane (red) or THF (blue) at 25 °C: [**P2**] = (a) 10 or (b) 1 mg mL^{-1}.

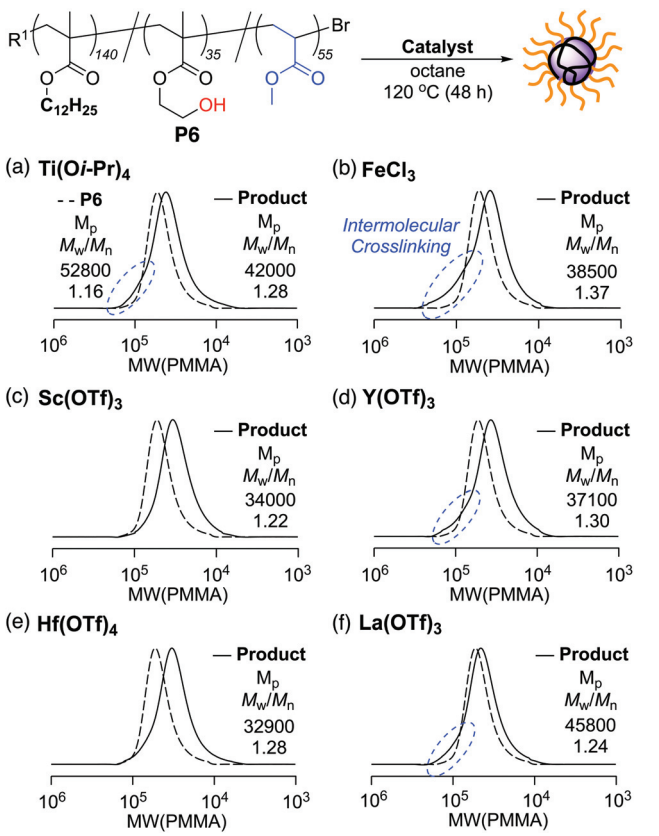

Fig. 2 SEC curves of the products (solid lines) obtained from the crosslinking of **P6** (dashed lines) with (a) $Ti(Oi\text{-}Pr)_4$, (b) $FeCl_3$, (c) $Sc(OTf)_3$, (d) $Y(OTf)_3$, (e) $Hf(OTf)_4$, and (f) $La(OTf)_3$ in octane at 120 °C for 48 h: $[P6]_0$ = 0.23 mM (10 mg mL^{-1}), $[catalyst]_0$ = 1.0 mM.

Table 2 Synthesis and characterization of crosslinked polymers[a]

Entry	Precursor	$[Polymer]_0$ (mg mL^{-1})	M_n [b] (SEC)	M_w/M_n [b] (SEC)	$M_p/M_{p,Precursor}$ [b] (SEC)	M_w [c] (MALLS)	MA Conv.[d] (%)
1	**P1**	10	39 800	1.15	0.64	83 900	35
2	**P2**	10	31 000	1.14	0.63	73 000	35
3	**P2**	50	41 600	1.21	0.73	87 500	30
4	**P2**	100	55 200	1.50	0.76	168 500	25
5	**P3**	10	27 200	1.13	0.71	46 600	30
6	**P4**	10	13 700	1.10	0.73	24 100	40
7	**P5**	10	20 400	1.15	0.63	38 900	n.d.
8	**P6**	10	28 100	1.22	0.64	69 800	40
9	**P7**	10	24 800	1.66	0.60	—	n.d.
10	**P7**	1	14 600	1.50	0.46	33 400	n.d.
11	**P8**	10	16 200	1.80	0.58	—	20
12	**P8**	1	9300	1.30	0.50	18 300	30

[a] Conditions: $[polymer]_0$ = 0.03–1.88 mM (1–100 mg mL^{-1}), $[Sc(OTf)_3]_0$ = 1.0 mM in (entries 1–6, 8) octane, (entry 7) octane/anisole (1/1, v/v), and (entries 9–12) anisole at 120 °C for 48 h. [b] Determined by SEC in THF with PMMA standard calibration. [c] Absolute weight-average molecular weight determined by SEC-MALLS in THF. [d] MA conversion determined by ^{1}H NMR. n.d.: not determined.

bility of the catalysts in octane, and association of the catalysts to the polymer pendants.

In addition to the selection of catalysts, the removal of MeOH generated from the transesterification of polymers is also important to shift the equilibrium and enhance the reaction yield.[39,40,43] But in the systems using $Sc(OTf)_3$ or $Hf(OTf)_4$, transesterification effectively proceeded in the absence of molecular sieves for the removal of MeOH probably due to the relatively high reaction temperature of 120 °C.

Interestingly, $Ti(Oi\text{-}Pr)_4$ partially induced physical crosslinking *via* the coordination of the titanium metals onto the hydroxyl pendants,[21,22] in addition to chemical crosslinking *via* transesterification (Fig. S6†). This is confirmed by the following: after the removal of free $Ti(Oi\text{-}Pr)_4$ catalysts, a crosslinked **P6** was treated with benzyl alcohol in anisole at 120 °C for 48 h. The SEC peak-top molecular weight of the product slightly shifted to a high molecular weight, indicating that the ligand exchange of the entrapped titanium metals with benzyl alcohol occurred to cleave the in-core physical crosslinking.

Based on the catalyst survey, we decided to employ $Sc(OTf)_3$ for the intramolecular transesterification of methacrylate/acrylate copolymers. Preferential transesterification of MA units was further supported by the following model experiments. Transesterification of methyl pivalate or methyl isobutyrate (as model compounds of MMA or MA units) was conducted with $Sc(OTf)_3$ in toluene/benzyl alcohol (1/1, v/v) at 80 °C for 48 h (Fig. S3†). Confirmed by ^{1}H NMR, methyl isobutyrate as a model of MA was transesterified into a corresponding benzyl ester (61%) more efficiently than methyl pivalate as a model of MMA (41%). PMA (M_n = 6200, M_w/M_n = 1.08) was transesterified into benzyl ester pendants (16% conversion, by ^{1}H NMR) with $Sc(OTf)_3$ in anisole/benzyl alcohol (1/1, v/v) at 120 °C (48 h), while PMMA (M_n = 7600, M_w/M_n = 1.21) was not reacted (0% conversion) (Fig. S4†).

We thus investigated the synthesis of single-chain crosslinked polymers bearing octadecyl pendants *via* the intramolecular transesterification of ODMA/HEMA/MA random copolymers (**P1–P5**) with $Sc(OTf)_3$ in octane at 120 °C (Fig. 3), focusing on the effects of polymer structure, composition, degree of polymerization (DP), solvents, and concentration. **P2** (M_n = 53 300, M_w/M_n = 1.18, ODMA/HEMA/MA = 140/40/55, [**P2**] = 0.19 mM, 10 mg mL^{-1}) was treated with $Sc(OTf)_3$ (1.0 mM) in octane at 120 °C for 48 h (Fig. 3b). The SEC curve of the product clearly shifted to a low molecular weight, maintaining a narrow molecular weight distribution (M_w/M_n = 1.14). Confirmed by ^{1}H NMR measurement of the product (Fig. 3i and j), the methoxy protons of the MA units decreased (*g*: 3.7–3.5 ppm, 35% conversion), whereas the methylene protons of ODMA units adjacent to the ester units did not decrease as much (*a*: 4.05–3.85 ppm, 10% conversion). Additionally, the methylene protons of HEMA units (*e*: 4.2–4.05, *f*: 3.85–3.7 ppm) decreased and turned broad. These results support that the MA units are consumed more selectively than ODMA (methacrylate) units *via* intramolecular transesterification with the HEMA hydroxyl groups. The absolute weight-average molecular weight (M_w) of the product was determined to be 73 000 by SEC-MALLS (Table 2). The M_w value was close to that of **P2** (M_w = 67 700), indicating that **P2** was unimolecularly crosslinked within a reverse micelle in octane.

The catalyst and MA and HEMA units were required for efficient intramolecular transesterification (Fig. S7†). **P2** without using $Sc(OTf)_3$ or an ODMA/MA random copolymer (**P9** without hydroxyl groups, M_n = 49 700, M_w/M_n = 1.11, ODMA/MA = 160/45) with $Sc(OTf)_3$ was not transesterified at all (no SEC peak shift, no MA consumption). Hydroxyl-bearing all methacrylate copolymers (**P10**: M_n = 30 600, M_w/M_n = 1.18, ODMA/HEMA = 75/30, **P11**: M_n = 38 800, M_w/M_n = 1.10, ODMA/HEMA/MMA = 90/35/35) induced transesterification with $Sc(OTf)_3$ (1.0 mM) in octane at 120 °C, whereas the consumption of ODMA and MMA units was 10%–20% at most. The SEC peak shift of the crosslinked products of **P10** and **P11** to a low molecular weight ($M_p/M_{p,precursor}$ = ~0.7) was smaller than that of **P2** ($M_p/M_{p,precursor}$ = 0.63).

Reverse micellization of **P2** in octane is also important for the intramolecular crosslinking of polymers at a relatively high concentration. In fact, **P2** preferentially induced unimolecular

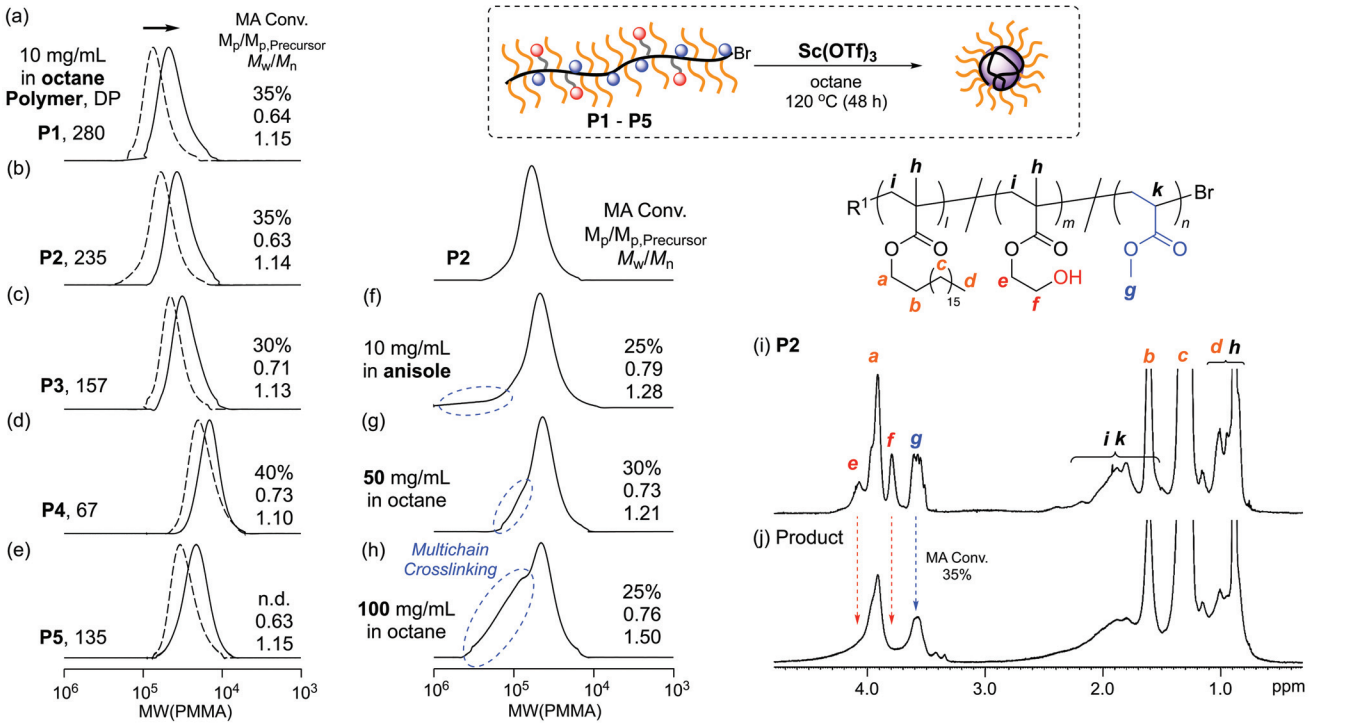

Fig. 3 SEC curves of the products obtained from the transesterification crosslinking of (a) **P1**, (b, f, g, h) **P2**, (c) **P3**, (d) **P4**, and (e) **P5** in (a–d, g, h) octane, (e) octane/anisole (1/1, v/v), and (f) anisole at 120 °C for 48 h (a–e, dashed lines: **P1**–**P5**, solid lines: products): [polymer] = 10 mg mL^{-1} [(a) 0.16, (b, f) 0.19, (c) 0.25, (d) 0.60, (e) 0.35, (g) 0.95, (h) 1.9 mM], $[Sc(OTf)_3]_0$ = 1.0 mM. ^1H NMR spectra of (i) **P2** and (j) the product obtained from the condition (b) in CD_2Cl_2 at 25 °C.

crosslinking up to 50 mg mL^{-1} in octane (Fig. 3g) and homogeneously crosslinked even at 100 mg mL^{-1} without any macroscopic gelation (Fig. 3h). In contrast, the product obtained in anisole (10 mg mL^{-1}) did not turn compact and contained multichain crosslinked fractions in the high molecular weight region (Fig. 3f and S8†).

Transesterification of ODMA/HEMA/MA random copolymers (**P1**, **P3**–**P5**) was conducted with $Sc(OTf)_3$ in octane at 120 °C. The polymer concentration was kept as 10 mg mL^{-1}. In all the cases, the copolymers were transesterified to give crosslinked polymers with a narrow molecular weight distribution, independent of DP and composition (Fig. 3a–e and S9†). Determined by SEC-MALLS, the absolute weight-average molecular weight (M_w) of the products was close to that of the corresponding precursors: M_w (products)/M_w (precursors) = 1.0–1.3 (Tables 1 and 2). This is indicative of the preferential synthesis of single-chain crosslinked polymers. It should be noted that this crosslinking system affords the precise and direct control of the molecular weight of the crosslinked polymers by tuning the DP of the precursors. **P5** had a content of the linking units ($m + n$ = 67 mol%) higher than the others (*e.g.*, **P3**: $m + n$ = 39 mol%). Thus, in the case of an almost identical DP, the crosslinked **P5** turned more compact than the crosslinked **P3**, as confirmed by the ratio of the peak-top molecular weight of the products and the precursors [$M_p/M_{p,Precursor}$ = 0.63 (**P5**), 0.71 (**P3**)]. The molecular weight of the crosslinked **P1** did not change even after the treatment with benzyl alcohol at 120 °C. This supports that $Sc(OTf)_3$ does not induce physical crosslinking by coordination of the metals to polymer pendants like $Ti(Oi\text{-}Pr)_4$.

In contrast to **P1**–**P6**, MMA or MA-based copolymers (**P7**, **P8**) were not soluble in octane. Thus, transesterification of **P7** and **P8** was examined with $Sc(OTf)_3$ in anisole at 120 °C (Fig. 4). The polymer concentration was set as 10 or 1 mg

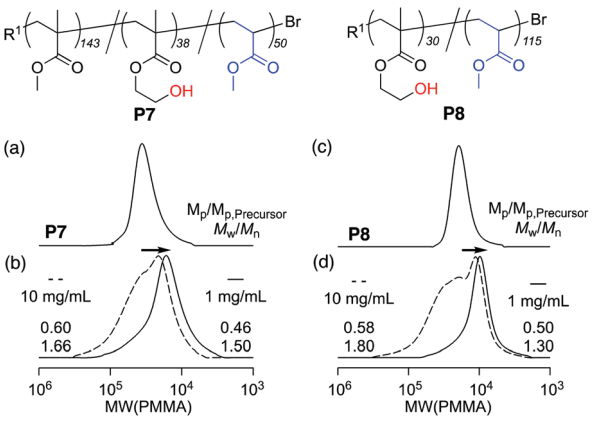

Fig. 4 SEC curves of (a) **P7**, (c) **P8**, and the products obtained from the transesterification crosslinking of (b) **P7** or (d) **P8** in anisole at 120 °C for 48 h: [polymer] = 10 (dashed lines) or 1 (solid lines) mg mL^{-1} [(b) 0.3 or 0.035 mM, (d) 0.59 or 0.059 mM], $[Sc(OTf)_3]_0$ = 1.0 mM.

mL^{-1}. At 1 mg mL^{-1}, both **P7** and **P8** preferentially induced intramolecular transesterification to form compact and crosslinked polymers, respectively (Table 2). In contrast, large amounts of multichain crosslinked polymers were formed at 10 mg mL^{-1}, in addition to single-chain crosslinked polymers. These results indicate that, at a low polymer concentration (~1 mg mL^{-1}), Sc(OTf)$_3$-mediated transesterification is applicable to the preparation of various crosslinked polymer nanoparticles without using reverse micellization.

The structure of crosslinked **P3** or **P5** was evaluated by intrinsic viscosity and light scattering measurements coupled with SEC. The intrinsic viscosity ([η]) of **P3**, **P5**, and their crosslinked products increased with molecular weight. In both cases, the intrinsic viscosity of the crosslinked products decreased against the corresponding precursors, indicating that the crosslinked polymers have more compact structures than the precursors. The double logarithmic plots of intrinsic viscosity ([η]) *versus* molecular weight (M_w) were fitted using the Mark–Houwink–Sakurada equation ([η] = KM^{α}) (Fig. 5). The slope α of a crosslinked **P5** turned out to be 0.44, smaller than that of the other samples (α = ~0.65). This importantly means that the crosslinked **P5** forms a more globular structure in THF probably owing to the high density of crosslinking units.

The globular structures of crosslinked **P3** or **P5** were also supported by small-angle neutron scattering (SANS) measurements in THF-d_8 at 25 °C (Fig. 6). In the double logarithmic SANS profiles, the scattering intensity of both the crosslinked

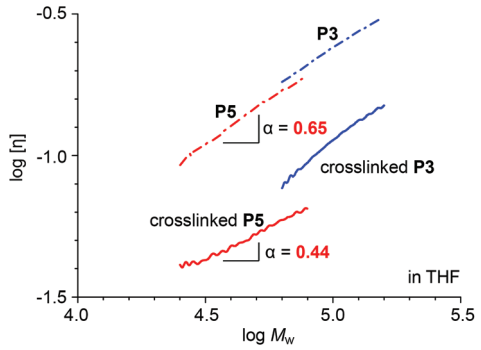

Fig. 5 Intrinsic viscosity of **P3** and **P5** and their crosslinked products (crosslinked **P3**, crosslinked **P5**) against molecular weight in THF.

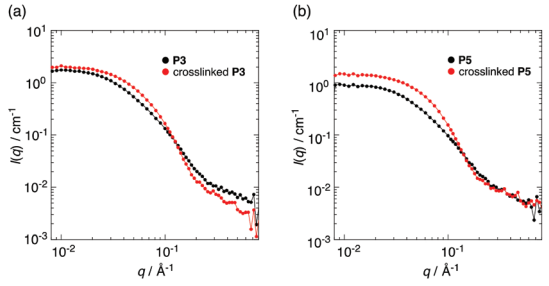

Fig. 6 SANS profiles of (a) **P3** and crosslinked **P3** and (b) **P5** and crosslinked **P5** in THF-d_8 at 25 °C: [polymer] = 10 mg mL^{-1}.

P3 and crosslinked **P5** at around 1 nm^{-1} of q decreased with increasing q in the slope of −4. Determined by the Guinier plots (Fig. S10†), the radius of gyration of their crosslinked products was smaller than that of the corresponding precursors [R_g = 4.2 nm (**P3**), 3.5 nm (crosslinked **P3**), 3.7 nm (**P5**), 3.2 nm (crosslinked **P5**)].

Crystallinity control by crosslinking

Octadecyl and long alkyl-bearing (co)polymers are interesting as crystalline materials.[38] Thus, the crystallinity of **P1–P4** was evaluated by differential scanning calorimetry (DSC), focusing on the crosslinking degree, DP, and composition of the polymers. To investigate the effects of crosslinking degree on the crystallization of the octadecyl groups, we sampled products with different MA conversions from the transesterification of **P2** in octane in predetermined periods. The products obtained at 0.5, 1.0, 2.0, 4.0, 8.0, 24, and 48 h were analyzed by SEC and ^{1}H NMR (Fig. 7a,b and S11, Table S2†). The SEC curves of the products gradually shifted to low molecular weight, keeping a narrow molecular weight distribution, as the reaction time increased. Confirmed by ^{1}H NMR, the MA units were also gradually consumed up to 35%. Thus, crosslinked polymers gradually turned compact as the MA units were consumed by transesterification.

The products were analyzed by DSC. The solid samples were obtained from the evaporation of the dichloromethane solutions of the polymers, followed by drying *in vacuo*. To erase the thermal history, the samples were first heated to 150 °C and then cooled to −80 °C and again heated to 150 °C; the heating or cooling rate was set to 10 °C min^{-1}. The DSC thermograms recorded for the first cooling scans and the second heating scans are shown in Fig. 7c and d, respectively. All the products showed exothermic and endothermic peaks originating from the crystallization and melting of the octadecyl pendants, respectively. The exothermic and endothermic peaks of the products gradually turned broad as the intramolecular crosslinking proceeded. The melting or crystalline temperature (T_m, T_c) and their enthalpies decreased with increasing MA conversion (*e.g.*, **P2**: T_m = 33 °C, crosslinked **P2**: T_m = 32–26 °C, Fig. 7e). This indicates that the crystallinity of the octadecyl groups gradually decreases as the intramolecular crosslinking of **P2** proceeds.

The crosslinked products were further examined by X-ray diffraction (Fig. 7f). **P2** showed a sharp peak derived from the hexagonal packing of the octadecyl groups at a 2θ value of 21° (*d*-spacing = 4.2 Å).[38] The sharp peaks gradually decreased and amorphous halo peaks were observed as the crosslinking reaction proceeded. These results suggest that, with increasing intramolecular crosslinking, the polymers lose the ability to arrange the side chains suitable for crystallization. The crystallization of these polymers originates from the intermolecular and intramolecular association of the octadecyl groups.

Other crosslinked polymers of **P1–P4** also showed broad crystalline and melting peaks of the octadecyl pendants with

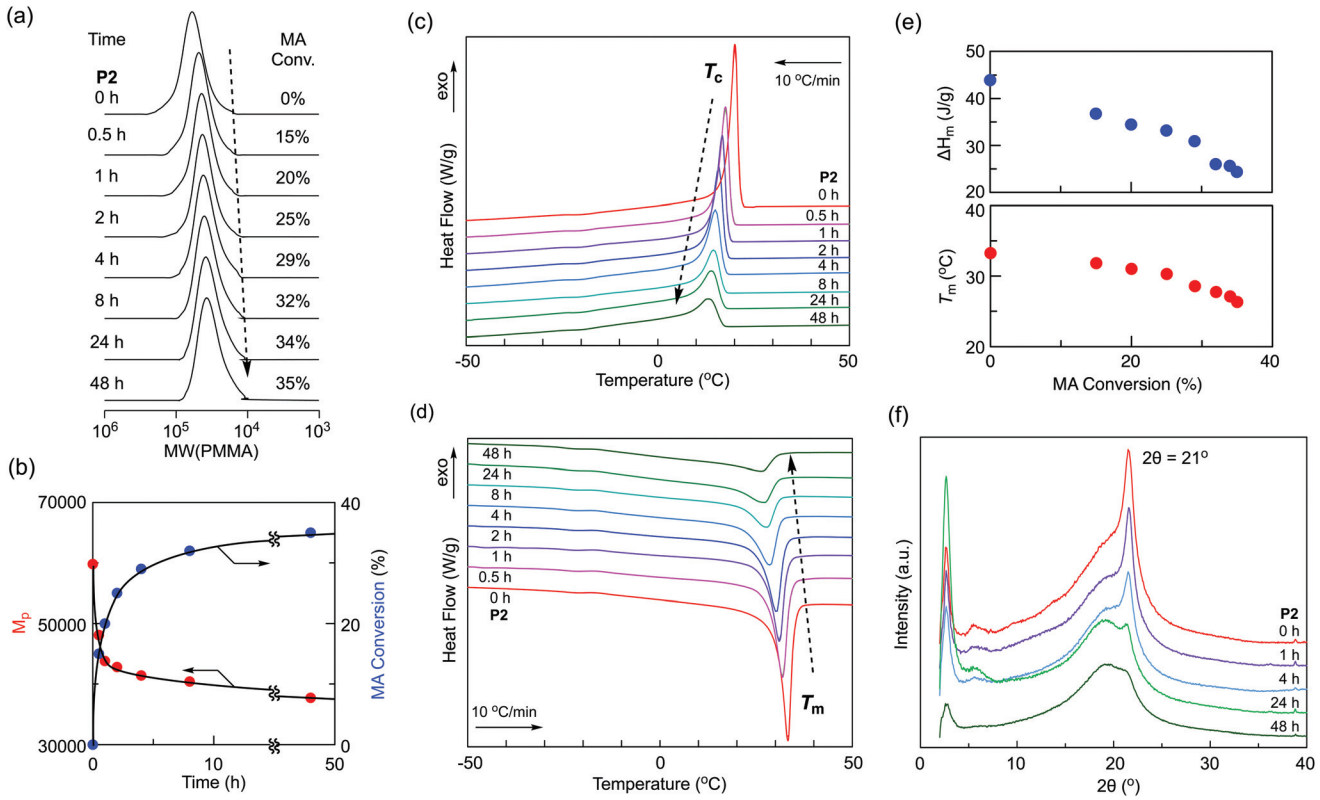

Fig. 7 Crystallization behavior of the products obtained from the intramolecular crosslinking of **P2** in octane at 120 °C. (a) SEC curves of the products obtained at various reaction times (0, 0.5, 1, 2, 4, 8, 24, and 48 h). (b) SEC peak top molecular weight and MA conversion of the products against reaction time. (c, d) DSC thermograms of the products obtained from (c) cooling or (d) heating scans between −80 °C and 150 °C: heating/cooling rate = 10 °C min^{-1}. (e) Melting temperature (T_m) and enthalpy of melting (ΔH_m) for the octadecyl units of the products against reaction time. (f) X-ray diffractograms of the products.

Table 3 Melting and crystallization temperatures and enthalpy

Entry	Polymer	T_m [a] (°C)	ΔH_m [a] (J g^{-1})	T_c [a] (°C)	ΔH_c [a] (J g^{-1})
1	**P1**	33.6	39.0	19.6	39.0
2	Crosslinked **P1** (10 mg mL^{-1})	23.3	23.2	11.9	23.3
3	**P2**	33.3	43.9	20.1	44.2
4	Crosslinked **P2** (10 mg mL^{-1})	26.3	24.4	13.2	24.4
5	Crosslinked **P2** (50 mg mL^{-1})	30.1	34.1	16.5	33.7
6	Crosslinked **P2** (100 mg mL^{-1})	30.4	34.6	16.8	34.9
7	**P3**	33.8	38.7	20.0	38.7
8	Crosslinked **P3** (10 mg mL^{-1})	26.8	25.4	13.8	25.4
9	**P4**	33.9	44.9	20.9	45.2
10	Crosslinked **P4** (10 mg mL^{-1})	27.6	25.3	14.5	25.4

[a] Melting and crystallization temperatures (T_m, T_c) and the enthalpy of melting and crystallization (ΔH_m, ΔH_m) were determined by differential scanning calorimetry (DSC). The heating and cooling rates were 10 °C min^{-1} and −10 °C min^{-1}, respectively, between −80 °C and 150 °C. The polymer samples of the entries 2, 4, 5, 6, 8, and 10 correspond to the samples of entries 1, 2, 3, 4, 5, and 6 in Table 2.

lower T_c and T_m than the corresponding precursors (Table 3, Fig. S12†). In these samples, T_m of the octadecyl pendants depended on the crosslinking degree (*i.e.*, MA conversion). T_m of **P2** crosslinked at 50 or 100 mg mL^{-1} for 48 h (T_m = ~30 °C) was close to T_m of **P2** crosslinked at 10 mg mL^{-1} for 2 h; the MA conversion for those samples was around 25%–29%. T_m of the crosslinked **P1**–**P4** with 30%–40% MA conversion ranged from 23 °C to 27 °C. Therefore, intramolecular crosslinking of octadecyl pendant copolymers is regarded as a strategy to control crystallinity and thermal properties.

Conclusions

In conclusion, we produced single-chain crosslinked polymers with controlled crystallization properties by the intramolecular

transesterification of random copolymers comprising octadecyl methacrylate, 2-hydroxyethyl methacrylate, and methyl acrylate in octane. Their efficient synthesis involves crosslinking of self-folded reverse unimer micelles in organic solution, where the methyl acrylate units are selectively transesterified with the hydroxyl groups. This system enables us to control the molecular weight of the crosslinked polymers as desired because the molecular weight corresponds to that of the precursors that are precisely synthesized by living radical polymerization. The crystallinity of the polymer materials can also be controlled by the crosslinking degree. Thus, this work opened a way to produce well-defined polymer nanoparticles and crystallinity-controlled polymers that would be useful as functional materials and additives for surface coating, painting, optical plastics, and cosmetics, among many others.

Conflicts of interest

There are no conflicts to declare.

Acknowledgements

This work was supported by the Japan Society for the Promotion of Science KAKENHI Grant Numbers JP17H03066, JP17K19159, JP19K22218, and JP20H02787, by The Ogasawara Foundation for the Promotion of Science & Engineering, by The Noguchi Institute, by Inamori Foundation, and by Tokuyama Science Foundation. The SANS measurement was performed on BL15 at the Materials and Life Science Experimental Facility of the J-PARC (Proposal No. 2018B0092, 2019A0312, 2019B0089). We also thank Dr. Shin-ichi Takata (J-PARC) for the experimental support of the SANS measurements.

Notes and references

1 J. M. Ren, T. G. McKenzie, Q. Fu, E. H. H. Wong, J. Xu, Z. An, S. Shanmugam, T. P. Davis, C. Boyer and G. G. Qiao, *Chem. Rev.*, 2016, **116**, 6743–6836.
2 K. Matyjaszewski and N. V. Tsarevsky, *J. Am. Chem. Soc.*, 2014, **136**, 6513–6533.
3 T. Terashima, *Polym. J.*, 2014, **46**, 664–673.
4 H. Gao, *Macromol. Rapid Commun.*, 2012, **33**, 722–734.
5 A. Blencowe, J. F. Tan, T. K. Goh and G. G. Qiao, *Polymer*, 2009, **50**, 5–32.
6 H. Gao and K. Matyjaszewski, *Prog. Polym. Sci.*, 2009, **34**, 317–350.
7 T. Shibata, S. Kanaoka and S. Aoshima, *J. Am. Chem. Soc.*, 2006, **128**, 7497–7504.
8 Y. Koda, T. Terashima and M. Sawamoto, *J. Am. Chem. Soc.*, 2014, **136**, 15742–15748.
9 M. Talelli, M. Barz, C. J. F. Rijcken, F. Kiessling, W. E. Hennink and T. Lammers, *Nano Today*, 2015, **10**, 93–117.
10 M. Elsabahy, G. S. Heo, S. M. Lim, G. Sun and K. L. Wooley, *Chem. Rev.*, 2015, **115**, 10967–11011.
11 A. O. Moughton, M. A. Hillmyer and T. P. Lodge, *Macromolecules*, 2012, **45**, 2–19.
12 M. Elsabahy and K. L. Wooley, *J. Polym. Sci., Part A: Polym. Chem.*, 2012, **50**, 1869–1880.
13 R. K. O'Reilly, C. J. Hawker and K. L. Wooley, *Chem. Soc. Rev.*, 2006, **35**, 1068–1083.
14 T. Terashima, *ACS Symp. Ser.*, 2018, **1285**, 143–155.
15 S. Mavila, O. Eivgi, I. Berkovich and N. G. Lemcoff, *Chem. Rev.*, 2016, **116**, 878–961.
16 O. Altintas and C. Barner-Kowollik, *Macromol. Rapid. Commun.*, 2016, **37**, 29–46.
17 M. Gonzalez-Burgos, A. Latorre-Sanchez and J. A. Pomposo, *Chem. Soc. Rev.*, 2015, **44**, 6122–6142.
18 A. M. Hanlon, C. K. Lyon and E. B. Berda, *Macromolecules*, 2016, **49**, 2–14.
19 T. Mes, R. van der Weegen, A. R. A. Palmans and E. W. Meijer, *Angew. Chem., Int. Ed.*, 2011, **50**, 5085–5089.
20 N. Hosono, M. A. J. Gillissen, Y. Li, S. S. Sheiko, A. R. A. Palmans and E. W. Meijer, *J. Am. Chem. Soc.*, 2013, **135**, 501–510.
21 S. Mavila, I. Rozenberg and N. G. Lemcoff, *Chem. Sci.*, 2014, **5**, 4196–4203.
22 J. Willenbacher, O. Altintas, V. Trouillet, N. Knöfel, M. J. Monteiro, P. W. Roesky and C. Barner-Kowollik, *Polym. Chem.*, 2015, **6**, 4358–4365.
23 E. A. Appel, J. Dyson, J. del Barrio, Z. Walsh and O. A. Scherman, *Angew. Chem., Int. Ed.*, 2012, **51**, 4185–4189.
24 I. Perez-Baena, I. Asenjo-Sanz, A. Arbe, A. J. Moreno, F. L. Verso, J. Colmenero and J. A. Pomposo, *Macromolecules*, 2014, **47**, 8270–8280.
25 O. Altintas, J. Willenbacher, K. N. R. Wuest, K. K. Oehlenschlaeger, P. Krolla-Sidenstein, H. Giliemann and C. Barner-Kowollik, *Macromolecules*, 2013, **46**, 8092–8101.
26 P. G. Frank, B. T. Tuten, A. Prasher, D. Chao and E. B. Berda, *Macromol. Rapid Commun.*, 2014, **35**, 249–253.
27 A. E. Cherian, F. C. Sun, S. S. Sheiko and G. W. Coates, *J. Am. Chem. Soc.*, 2007, **129**, 11350–11351.
28 T. Terashima, T. Sugita and M. Sawamoto, *Polym. J.*, 2015, **47**, 667–677.
29 M. Matsumoto, T. Terashima, K. Matsumoto, M. Takenaka and M. Sawamoto, *J. Am. Chem. Soc.*, 2017, **139**, 7164–7167.
30 B. S. Murray and D. A. Fulton, *Macromolecules*, 2011, **44**, 7242–7252.
31 Y. Azuma, T. Terashima and M. Sawamoto, Self-Folding Polymer Iron Catalysts for Living Radical Polymerization, *ACS Macro Lett.*, 2017, **6**, 830–835.
32 C. Song, L. Li, L. Dai and S. Thayumanavan, *Polym. Chem.*, 2015, **6**, 4828–4834.
33 E. H. H. Wong and G. G. Qiao, *Macromolecules*, 2015, **48**, 1371–1379.
34 T. Terashima, T. Sugita, K. Fukae and M. Sawamoto, *Macromolecules*, 2014, **47**, 589–600.
35 Y. Hirai, T. Terashima, M. Takenaka and M. Sawamoto, *Macromolecules*, 2016, **49**, 5084–5091.

36 S. Imai, Y. Hirai, C. Nagao, M. Sawamoto and T. Terashima, *Macromolecules*, 2018, **51**, 398–409.
37 Y. Koda, T. Terashima and M. Sawamoto, *Macromolecules*, 2016, **49**, 4534–4543.
38 G. Hattori, M. Takenaka, M. Sawamoto and T. Terashima, *J. Am. Chem. Soc.*, 2018, **140**, 8376–8379.
39 D. Ito, Y. Ogura, M. Sawamoto and T. Terashima, *ACS Macro Lett.*, 2018, **7**, 997–1002.
40 Y. Ogura, T. Terashima and M. Sawamoto, *J. Am. Chem. Soc.*, 2016, **138**, 5012–5015.
41 K. Yoshida, S. Tanaka, T. Yamamoto, K. Tajima, R. Borsali, T. Isono and T. Satoh, *Macromolecules*, 2018, **51**, 8870–8877.
42 C. P. Easterling, T. Kubo, Z. M. Orr, G. E. Fanucci and B. S. Sumerlin, *Chem. Sci.*, 2017, **8**, 7705–7709.
43 Y. Ogura, T. Terashima and M. Sawamoto, *Polym. Chem.*, 2017, **8**, 2299–2308.
44 J. Otera, *Chem. Rev.*, 1993, **93**, 1449–1470.
45 K. Ishihara, M. Kubota, H. Kurihara and H. Yamamoto, *J. Am. Chem. Soc.*, 1995, **117**, 4413–4414.
46 K. Ishihara, M. Nakayama, S. Ohara and H. Yamamoto, *Tetrahedron*, 2002, **58**, 8179–8188.
47 M. Hatano, Y. Furuya, T. Shimmura, K. Moriyama, S. Kamiya, T. Maki and K. Ishihara, *Org. Lett.*, 2011, **13**, 426–429.